III International Conference on Particle-based Methods – Fundamentals and Applications
PARTICLES 2013
M. Bischoff, E. Oñate, D.R.J. Owen, E. Ramm & P. Wriggers (Eds)

CRYSTAL GROWTH AND SOLID-LIQUID INTERFACE IN NIZR ALLOY: LINKING MOLECULAR DYNAMICS AND PHASE-FIELD MODELING

MOHAMMED GUERDANE

Institute of applied Materials, Karlsruhe Institute of Technology
Haid-und-Neu-Str. 7, 76131 Karlsruhe
mohammed.guerdane@kit.edu, http://www.iam.kit.edu/zbs/Mitarbeiter_guerdane.php

Key words: MD simulations, phase-field model, multiscale modeling, solid-liquid interface ordering

Abstract. We address the question of whether and how atomistic molecular dynamics (MD) simulations can be used to calibrate macroscopic phase-field (PF) models, as hierarchical multiscale approaches usually proceed. We carry out a systematic consistency analysis by confronting results from MD with predictions of PF modeling in the case of the propagation of a planar $[\mathrm{Ni}_c\mathrm{Zr}_{1-c}]_{\mathrm{liquid}}$-$\mathrm{Zr}_{\mathrm{crystal}}$ interface during solidification and melting under chemical nonequilibrium conditions. Our study illustrates clearly that the PF approach is able to describe the same aspects of physics than MD, when the key physical parameters are transferred from the latter method to the former one. We use then this consistent MD/PF multiscale model to estimate quantitatively the influence of the in-plane solid-liquid interface ordering on the growth kinetics.

1 INTRODUCTION

The need for multiscale modeling is motivated by the fact that important phenomena in materials sciences and engineering often involve interactions between microscopic and macroscopic length and time scales [1, 2]. Considering the solidification process, for instance, solid-liquid interfaces are on the order of a few angstroms, whereas microstructural features are on the length of tens of micrometers. Time scales of solidification span from picoseconds for the typical atomic dynamics processes, taking place at the interface, to seconds needed for transport of heat and matter away from the interface. Understanding the physics of solidification over such disparate length and time scales, about ten orders of magnitude, represents one of the challenges of present materials sciences, for which new mathematical models and numerical simulations algorithms have to be developed. Plastic deformation and fracture are other multiscale problems because they are intrinsically atomistic phenomena, where dislocation dynamics and bond breaking, respectively, need to be captured.

Over the last two decades, the PF method has emerged as a powerful computational approach to model solidification processes and microstructure formation, such as dendritic evolution and order-disorder transition kinetics, on meso- and macroscopic scales [3]. The problem of sharp boundaries between phases is circumvented by making these boundaries spatially diffuse over some width ε with the help of a scalar field ϕ that distinguishes between the different phases. The PF method is one of the approaches which are expected to push forward the field of multiscale modeling. Scale-bridging efforts towards the molecular scale have been recently done by coupling the PF model to atomistic computational techniques [4, 5]. This coupling can be realized dynamically or in a static way. In the first approach, at every time step of the overall algorithm, well-defined quantities are exchanged or optimized. This approach is still computationally expensive and therefore possible only for selected problems. The static approach consists in calculating selected physical quantities by means of atomistic models and using these quantities as fixed parameters to calibrate the higher-scale PF model. This latter 'weak coupling' approach has been applied by Vaithyanathan *et al.* [4] to study the growth and coarsening of θ-precipitates in Al-Cu alloys. They showed how first-principles atomistics may be combined with PF modeling, with the mixed-space cluster expansion as an intermediate tool to bridge the scale from angstroms to microns.

The central challenge quantitative multiscale models face is to ensure that descriptions at all scale levels are consistent with each other. The need for consistency requires a coupling between the microscopic and macroscopic descriptions. Regarding this coupling, multiscale models have been classified into two categories: hierarchical and concurrent [2]. Hierarchical or serial coupling methods use fine scale model simulations to acquire material-defining input to be used in a coarser scale model. Concurent coupling models, which are more rigorous and conceptually appealing procedures in realizing the multiscale goal, link microscale and macroscale models together 'on-the-fly' in a combined model.

In the present work, we address the consistency topic for one of the promising multiscale methods, namely the hierarchical coupling approach that combines MD with PF simulations. Firstly, the consistency analysis will be achieved by detailed comparisons of quantitative predictions of the considered modeling methods for the growth and melting kinetics of a two-phase NiZr system out of chemical equilibrium. The MD simulations provide the physical quantities needed for the construction of the multiscale model. Of central importance are the bulk free energy and the solid-liquid interfacial free energy whose calculation requires the use of special methods.

In a second stage, we demonstrate how short-range order (SRO) in the bulk liquid could transform into a massive lateral ordering at the interface when commensurability is given between the building blocks of the liquid and the periodic potential of the crystal wall. The quantitative influence of this structure on the growth kinetics is investigated using the consistent MD/PF multiscale model calibrated before.

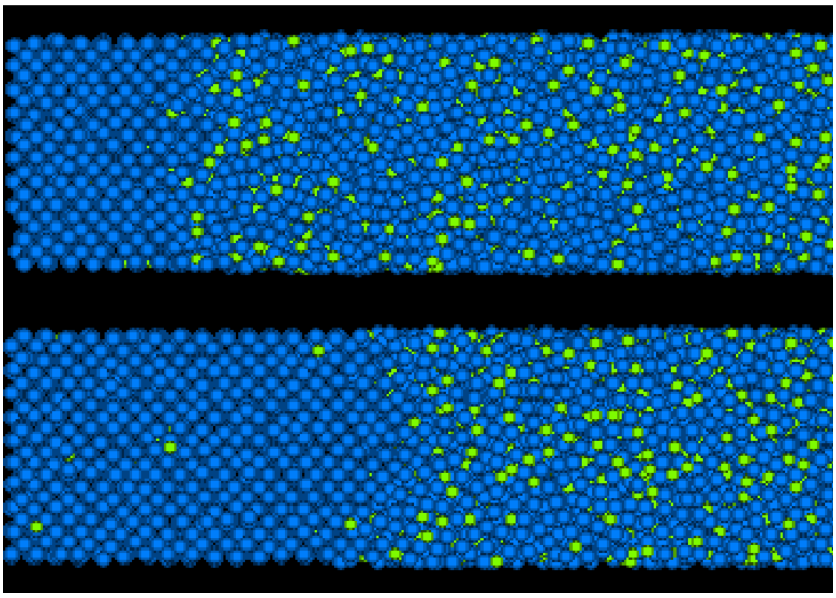

Figure 1: Top: Crystal-melt system equilibrated at $T = 1900$ K. Bottom: After cooling it down to $T = 1700$ K. Clearly visible is an expansion of the crystal, which implies an increase of the melt Ni-concentration after cooling (source: Ref. [6]).

2 MODELING METHODS

2.1 MD model

We perform MD simulations for an isothermal-isobaric (N, T, p) ensemble of N (up to about 10^6) particles and zero pressure. The parallelized MD program was designed, optimized, and extensively used in analyzing relaxation dynamics of NiZr and NiZrAl melts as well as crystallization kinetics in NiZr alloy ([6] and references therein).

Interatomic interactions are modeled by the sum of an electronic volume term plus short-ranged pair potentials. For the latter, a Stillinger-Weber form is used, adapted to first-principles interatomic interactions calculated by Hausleitner and Hafner for binary transition metal alloys [7].

All two-phase samples have a square cross section with a dimension of 10 times a, the lattice constant of bcc Zr. The crystal has a thickness of 20-50 times a, while a liquid-slab thickness of at least 1200 Å is needed to correctly simulate a diffusion-determined growth of 100 ns. Preparation of the two-phase sample, $\mathrm{Ni}_c\mathrm{Zr}_{1-c}$ melt in contact with bcc Zr, as well as the crystallization modeling are described in detail in our recent study [6].

Growth dynamics is studied by considering a crystal-liquid $[\mathrm{Ni}_c\mathrm{Zr}_{1-c}]_{liquid}$-$\mathrm{Zr}_{crystal}$ sample equilibrated at temperature T and brought into a non-equilibrium state by subjecting it to an abrupt negative temperature change ΔT. This corresponds in our case to an undersaturated solution at temperature $T+\Delta T$. During the subsequent relaxation process at $T+\Delta T$, the system moves in the direction of the equilibrium state by growing its bcc

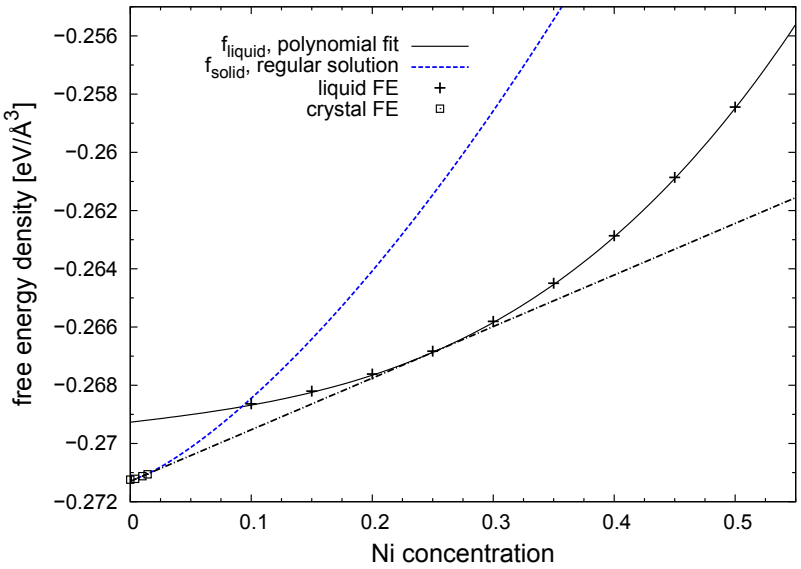

Figure 2: Crosses: MD-calculated free energy for Ni_cZr_{1-c} melts at $T = 1700$ K, the solid line is a third-order polynomial interpolation. Squares: free energy for bcc Zr at low Ni concentrations, the dashed line is an extrapolation according to the regular solution model. The dashed-dotted line is the double tangent (from Ref. [6])

Zr part (see Fig. 1). Thereby, the Ni concentration of the melt increases until the new equilibrium concentration is reached according to the liquidus line of the phase diagram given in Ref. [6]. All the solidification simulations considered in this study start from a layer sample equilibrated at temperature T=1900 K with an equilibrium concentration of the bulk liquid of c_l(1900 K)=0.219(3).

2.2 Calculating free energy and entropy of binary alloys from MD simulations

Understanding of the crystallization process of alloy melts requires the knowledge of the chemical potentials of the involved phases, as they are the driving forces for a phase transition. This means that we need to determine the temperature and concentration dependent free energy (FE) of the different phases. This task is not obvious for liquids by means of atomistic modeling, contrarely to crystals for which it is relatively easily tractable. In the following, we summarize the MD-based method developed in [8] to evaluate the free energy and the entropy of binary mixtures A_cB_{1-c}.

This method consists of two steps: (a) Calculation of entropy and free energy for two reference crystalline compositions using the quasi-harmonic approximation, (b) Calculation of entropy and free energy of A_cB_{1-c} melt for an arbitrary composition c using results of the reference systems in (a).

The crosses in Fig. 2 are FE values of Ni_xZr_{1-x} melts at $T = 1700$ K, as evaluated within this thermodynamic MD-based approach. The figure includes the FE of the bcc

Zr crystal at very low Ni concentrations (squares).

2.3 Phase-field model

Different from sharp-interface models of phase transitions, continuously varying order parameters $\phi_\alpha(\boldsymbol{r}, t)$ are introduced in the phase-field method. They describe the local volume fraction of the phase associated with the parameter, i.e. $\phi_\alpha = 1$ corresponds to a pure α phase, whereas the diffuse interface between two phases is characterized by $0 < \phi_\alpha < 1$. For this work, we use the thermodynamically consistent multi-phase field model given in detail in [9], for which many analytical, numerical and data postprocessing methods have been developed in our group. Evolution equations for the phase fields and concentrations are derived from the entropy functional defined on the spatial domain Ω

$$\mathcal{S} = \int_\Omega \Big(s(\boldsymbol{\phi}, \boldsymbol{c}, T) - \varepsilon a(\boldsymbol{\phi}, \nabla\boldsymbol{\phi}) - \frac{1}{\varepsilon} w(\boldsymbol{\phi}) \Big) d\boldsymbol{r}, \tag{1}$$

which contains separate bulk contributions $s(\boldsymbol{\phi}, \boldsymbol{c}, T)$ as a function of phase state, composition and temperature and interfacial entropy density contributions $a(\boldsymbol{\phi}, \nabla\boldsymbol{\phi})$ and $w(\boldsymbol{\phi})$, which depend only on the phase-field parameters. ε is a length related to the diffuse interface width. For the case of a binary system AB, we reduce the number of field variables to the sets $\boldsymbol{\phi} = (\phi_s, \phi_l)$ and $\boldsymbol{c} = (c_1, c_2)$ (1 for component A, 2 for component B), bearing in mind the constraints $\phi_l + \phi_s = 1$ and $c_1 + c_2 = 1$. Using the fundamental relation $e = f + Ts$ between internal energy density e, Helmholtz free energy density f and entropy density s, we obtain by differentiation: $\partial s/\partial e = 1/T$ and $\partial s/\partial c_i = -\mu_i/T$, where $\mu_i = \frac{\partial f}{\partial c_i}$. A general approach is to interpolate the free energy between the two phases in the form

$$f(\boldsymbol{\phi}, \boldsymbol{c}, T) = f_s(c_1, T)\, h(\phi_s) + f_l(c_1, T)\, h(\phi_l) = f_l(c_1, T) + (f_s(c_1, T) - f_l(c_1, T))\, h(\phi_s), \tag{2}$$

where $f_\alpha(c, T)$ is the c- and T-dependent free energy density of the phase α. The function $h(\phi)$ is a suitable interpolation function, for which we often use the polynomial $h(\phi) = \phi^2(3 - 2\phi)$.

The evolution equations are derived by variational differentiation of the entropy functional $\mathcal{S}(\boldsymbol{\phi}, \boldsymbol{c}, T)$, ensuring energy and mass conservation and the increase of total entropy. They read:

$$\partial_t c_1 = -\nabla \cdot \Big[L_{10}(\phi_l, c_1, T) \nabla \frac{1}{T} + \frac{1}{T} L_{11}(\phi_l, c_1, T)\, \nabla\big(\mu_2(\phi_l, c_1, T) - \mu_1(\phi_l, c_1, T)\big) \Big]. \tag{3}$$

$$\varepsilon\tau\partial_t\phi_s = \frac{\gamma}{T}\varepsilon\nabla^2\phi_s - \frac{1}{\varepsilon}\frac{\partial w(\phi_s)}{\partial\phi_s} - \frac{1}{2T}(f_s - f_l)\frac{\partial h(\phi_s)}{\partial\phi_s}. \tag{4}$$

The mobility coefficients L_{ij} obey the Onsager relation and define a symmetric matrix $L_{ij} = L_{ji}$. Owing to the constraint $\sum_i c_i = 1$, they also have the following summation property $L_{11} + L_{12} = 0$. Phase dependent diffusivities of the species i are interpolated using the previously defined interpolation function $h(\phi)$ as

$$D_i(\boldsymbol{\phi}) = D_i^s\, h(\phi_s) + D_i^l\, h(\phi_l), \tag{5}$$

where D_i^s and D_i^l are the diffusion coefficients of bulk solid and liquid, respectively. We determine the one-dimensional diffusion coefficients in liquid and solid by monitoring the asymptotic limit of the mean-square displacement in x direction, as described in Ref. [6]. This calculations yield: $D_{Ni,liq} = 1.74$, $D_{Zr,liq} = 0.893$, $D_{Ni,sol} = 15.30$, $D_{Zr,sol} = 10^{-3}$ (units in 10^{-9} m^2/s).

The gradient entropy density in Eq. (1) has been chosen as $a(\nabla\phi_s) = \sigma\,|\nabla\phi_s|^2$ and the potential in the form of a multi-well $w(\phi_s) = 9\sigma\,\phi_s^2(1-\phi_s)^2$. The parameter σ is the solid-liquid interfacial free energy. τ is a kinetic coefficient that has to be determined for a reference system. The nonlinear PDEs are solved numerically on a regular grid using a finite difference scheme with explicit time discretization, cyclic boundary conditions, and efficient parallel algorithms.

The interface width 2ϵ is estimated by using the local order parameter Q_6 because of its high sensitivity in discriminating crystalline and liquid atomic environment. This analysis yields the interface thickness $2\epsilon \simeq 12$ Å. Further details can be found in [6].

Due to the fact that in the present case the growth kinetics is diffusion controlled, there is no need to accuratly determine σ for $\mathrm{Zr}_{crystal}$-$[\mathrm{Ni}_x\mathrm{Zr}_{1-x}]_{liquid}$ interfaces. A value typical of a Zr-rich NiZr alloy would be largely sufficient. The only one known in the literature is that of pure Zr with $\sigma = 0.16$ J/m^2, that we use in our PF simulations.

3 RESULTS

Fig. 3 displays the evolution in time of the front position at T=1700 K after undercooling the sample from $T = 1900$ K, for both modeling methods. Fig. 4 compares the corresponding Ni-concentration profiles after 20 ns of the solidification process. The agreement between MD and PF modeling (thick and thin solid line, respectively) is very satisfactory. A good matching concerns also the solute concentrations in liquid at the interfaces, $c_{l,I}^{MD} = 0.250$ and $c_{l,I}^{PF} = 0.246$, both correspond to the equilibrium concentration values of the respective modeling method at 1700 K. The slightly slower solidification rate in PF simulation may be partly explained by the small discrepancy between the equilibrium liquid concentration realized in MD simulations, $c_l^{MD}(1700\text{ K}) = 0.250$, and that following from the calculated FE, $c_l(1700\text{ K}) = 0.246$, by means of the double tangent construction. As a consequence, the concentration peak height at the interface (liquid side) during solidification in Fig. 4 is about 13% smaller in PF simulations than in MD ones. This means a smaller gradient of the chemical potential at the solidification front, and thus a slower solidification kinetics. The PF approach gives the possibilty to verify this assumption, since we can 'by hand' shift the liquid FE curve vertically upwards so that the calculated equilibrium liquid concentration c_l matches with the MD one c_l^{MD}. Using the shifted liquid FE function in the PF simulation leads indeed to a better matching between PF and MD modeling, as illustrated by the dotted line in Fig. 3.

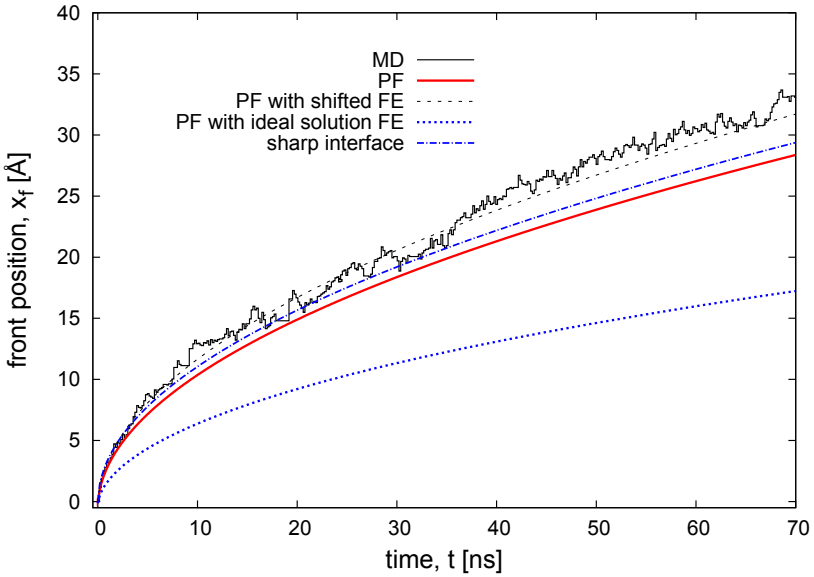

Figure 3: Interface position as a function of time during a solidification process of NiZr at T=1700 K, starting from a two-phase system equilibrated at T=1900 K. Compared are results from MD, PF and sharp interface models (source: Ref.[6]).

We conclude that MD simulations and PF modeling give the same quantitative physical description of the solidification kinetics in a crystal-liquid structure of NiZr alloy out of chemical equilibrium. Such a comparison is rendered possible after the PF model key parameters, on which the growth kinetics depends sensitively, are calculated within the MD approach. This equivalence test is important as it provides a legitimacy to the exchange of physical parameters between both modeling approaches when trying to bridge the gap between atomistic, mesoscopic and macroscopic scales. Further studies show that this conclusion concerns the melting kinetics as well [6]. Our study provides evidence that the applicability range of the continuum PF model extends down to the atomic level, without thermodynamic concepts loosing their relevance at this level. Moreover, thermodynamic and kinetic quantities -like the FE, the phase diagram, and the diffusivity- calculated for equilibrium conditions, seem to be a sufficient approximation for describing nonequilibrium situations.

The above agreement between MD and PF modeling concerns however only high temperatures (small undercooling). As the temperature decreases (high undercooling), an increasing deviation of the PF results from MD ones is observed, as shown in Fig. 5 (full squares). This deviation is traced back to the increasing confinement and ordering effect induced by the crystalline wall at the liquid side of the solid-liquid interface. This topic studied in our recent work [10] will be discussed in the following section.

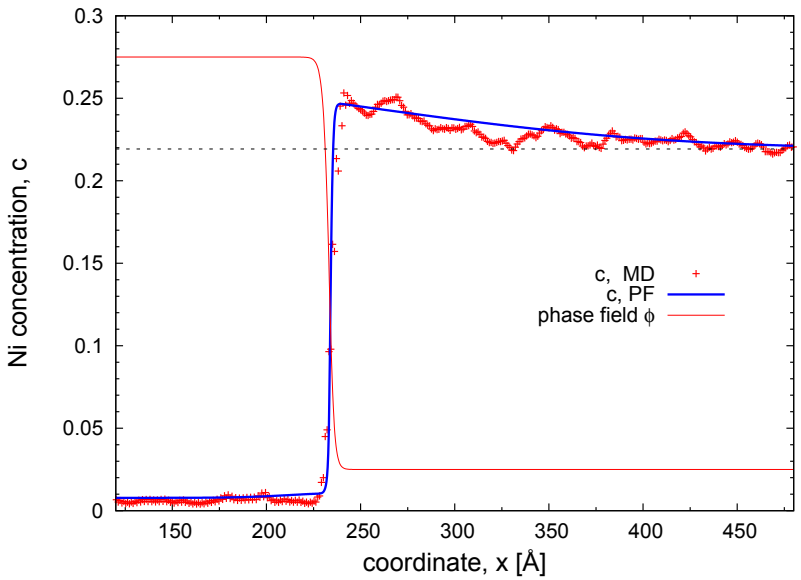

Figure 4: Ni-concentration profiles after 20 ns of a solidification process, from the same MD and PF simulations described in Fig. [3]. The dotted line indicates the initial equilibrium concentration c_l^0. The dashed line corresponds to the diffuse PF profile.

3.1 Hybrid MD/PF modeling to study the effect of interface ordering on the growth kinetics

Fig. 6 shows a side view of a solid-liquid interface. Each Ni atom is represented with its coordination polyhedron around. The interface exhibits a long-ranged translational order with structural units (SUs) arranged in a periodic pattern. The perpendicular (out of plane) order does not exceed the size of two SUs. A closer analysis of this ordered monolayer reveals that the SUs are in their majority Z9 polyhedra consisting of 9 Zr atoms surrounding a central Ni atom. These Zr atoms sit at the vertices of a trigonal prism (TP) capped with 3 half-octahedra at the square faces. One of the half-octahedra is shared with the bcc elementary cell of the Zr crystal (plane of Zr atoms '1' in Fig. 6. Alignment of the TPs at the crystal wall is clearly due to the commensurability of the TPs with the (100) faces of the bcc crystal. This conclusion is confirmed by analysis of other interface orientations. Starting with a perfectly flat (110) interface at 1100 K, it takes only some hundreds picoseconds for the interface to develop (100) facets and for the TPs in the melt to dock at this facets by adopting their orientation [10].

The energy profile at the interface in Fig. 7 (middle) shows that Ni atoms have a significantly lower energy at the ordered layer adjacent to the crystalline Zr wall than in the melt and in the solid. One expects that this relatively deep potential well of the interface will lead to a reduced mobility of the atoms laying in it. This is indeed what is seen in the in-plane diffusion profiles in Fig. 7 (bottom) describing slices with different distance from the interface: With reduced distance, when the crystal is approached from

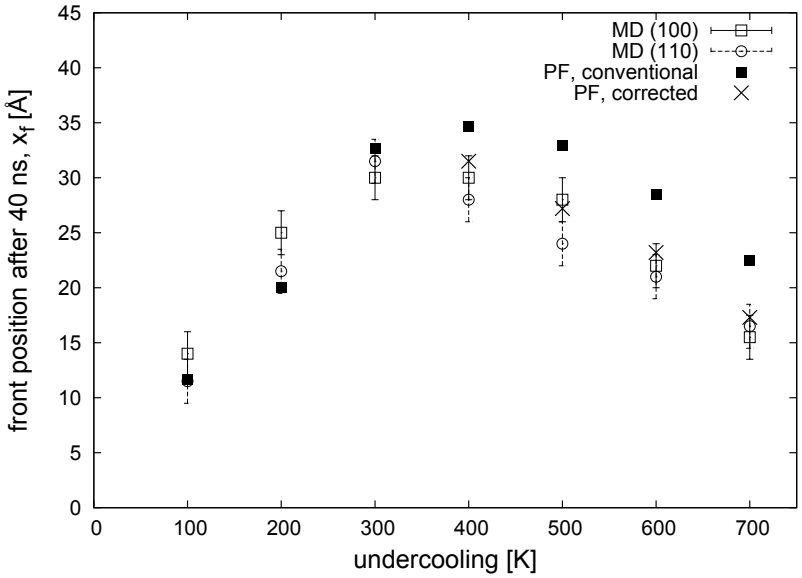

Figure 5: Front position x_f after 40 ns of solidification as a function of undercooling ΔT for MD and PF simulations. The initial temperature is $T = 1900$ K for all simulations (source: Ref.[10])

the melt, the mobility slows down continously because of the confining effect due to the "hard" wall. As the ordered Ni layer is reached, the Ni mobility drops abruptly (about 2 orders of magnitude) to a value comparable with that of vibrating Zr atoms in the crystal. We give here evidence that this high ordered Ni layer, albeit its SRO is reminiscent of that of the bulk liquid, is dynamically decoupled from the latter.

The interface ordering effect, manifesting itself as a diffusivity drop at the interface, has not been taken into account in the PF modeling. In the construction of the phase dependent diffusivity in Eq. 5, we made use of the standard method to interpolate the diffusion coefficients at the solid-liquid interface by means of a monotone interpolation function h. This conventional simple construction, which assume the same profile for the phase parameter ϕ and the diffusivity D, completely neglects the surface effect yielding to an overestimate of the growth rate relatively to the MD simulation.

A solution to incorporate the atomic interface ordering into the PF modeling is to use the complete diffusion profile determined from MD simulations. The decoupling of D from ϕ allows a realistic atomic representation of the diffusion in and around the interface in the PF model. This concept is justified in the present case by the fact that the growth kinetics is long-ranged-diffusion limited and, hence is dominated by the mass transport from the interface towards the bulk liquid. The increased ordering with decreasing undercooling is represented by the increasing diffusion drop at the interface. The crosses in Fig. 5 represent the results of PF modeling after using the diffusion profiles as calculated by MD simulations [6]. The agreement between PF and MD modeling regarding the growth rates at low temperatures is indeed reestablished.

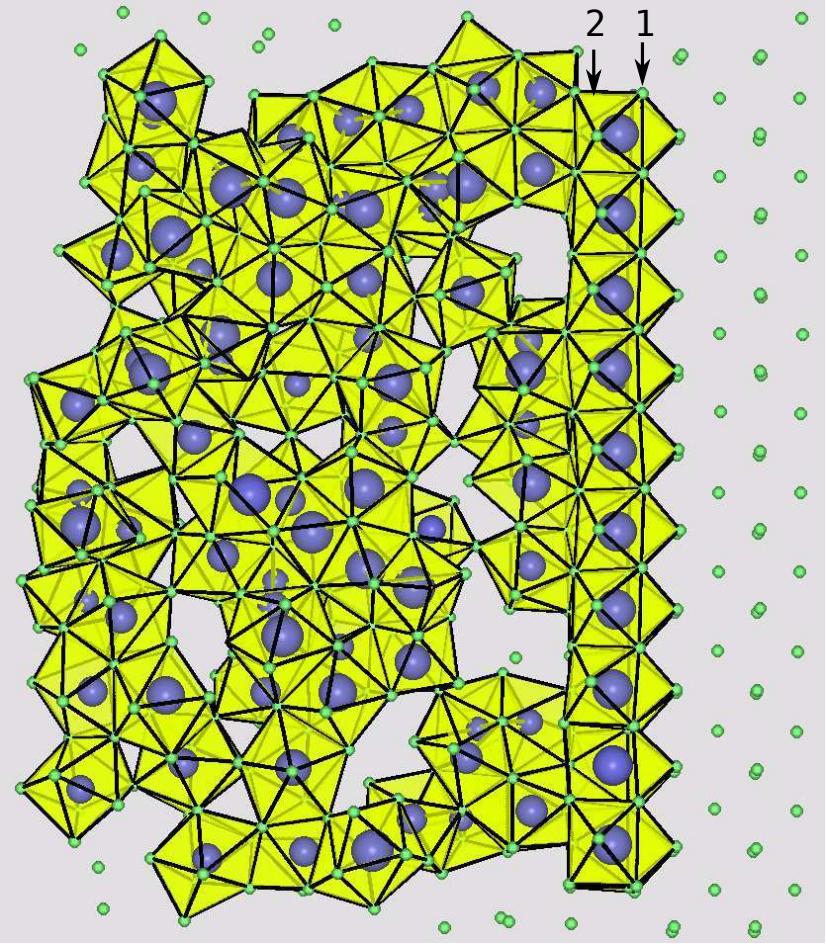

Figure 6: Side view of a $[Ni_cZr_{1-c}]_{liquid}$-$Zr_{crystal}$ (100) interface at 1100 K. For clarity, Zr atoms are represented by small spheres. Each Ni atom is represented by its coordination polyhedron. The Ni-atom size scales with the distance from the drawing plane. The number '1' and '2' designate two different Zr-atom planes (source: Ref.[10])

This hybrid MD/PF study of atomic ordering behaviour and the effect on the diffusion across liquid-solid interface illustrates very well how ordering in the melt could transform into a delaying factor of the crystallization. In the case of the homogeneous crystal nucleation, we found that Zr nuclei formed in the melt quickly develop (100) facets. Subsequently, the Zr nuclei become wetted by a NiZr melt shell of TPs with the effect of delaying or completely blocking the growth of these nuclei into the critical size. Our observations provide evidence for a strong link between the interface ordering and the SRO in the bulk liquid. In other words, what we observe are not only single 'liquid' atoms which mimic the periodicity of the crystalline wall without any relation to the local order of the melt, as reported until now in the literature. Rather, the liquid alloy rearranges the solid-liquid surface to develop (100) facets and then docks its trigonal

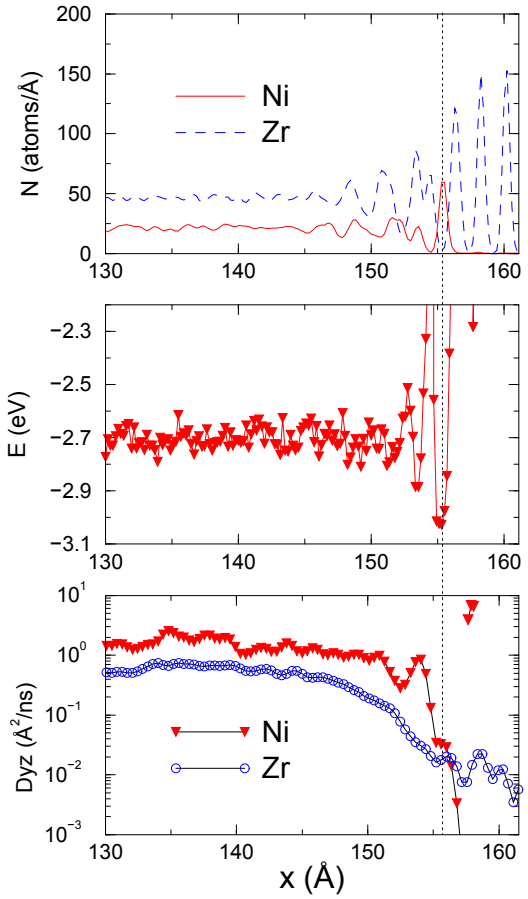

Figure 7: Top: One-dimentional Ni- and Zr-concentration profiles. Middle: Ni potential-energy profile. Bottom: Lateral (in-plane) diffusion profiles for Ni and Zr. All profiles are calculated bei averaging over several configurations near the time of the snapshot of Fig. 6. The vertical dashed line marks the position of the ordered interface layer which manifests itself with a pronounced peak in the Ni-concentration profile (source: Ref.[10]).

prisms at them. In this way, the interface unequivocally exhibits the signature of SRO of the melt and the medium-range order of the crystal. The quantitative influence of this interface effect on the growth kinetics is investigated by linking MD to PF modeling. 'Freezing' of the melt SRO at the interface is found to act against the crystallization. The finding of our study are of relevance for alloy growth kinetics as well as for the fundamental open question of local (atomic) structure of metallic liquid. Regarding the last point, we notice that there has been very rare attempts to give experimental proof for the existence of the coordination polyhedra of Kasper type predicted theoretically for metallic multicomponent melts. Direct observation of a characteristic geometrical local order (e.g., icosahedral clustering) in the melt have concerned rather pure metals. Our present work suggests to look for a specific Kasper polyhedron in the melt at solid-liquid

interfaces when this polyhedron type is commensurate with the periodic potential of the crystal.

REFERENCES

[1] J.J. de Pablo and W.A. Curtin, Multiscale modeling in advanced materials research: challenges, novel methods, and emerging applications. *MRS Bull.* (2007) **32**:905.

[2] W.A. Curtin and R.E. Miller, Atomistic/continuum coupling methods in multi-scale materials modeling. *Modeling Simul. Mater. Sci. Eng.* (2003) **11**:R33-R68.

[3] W.J. Boettinger, J.A. Warren, C. Beckermann, and A. Karma, Phase-field simulation of solidification. *Annu. Rev. Mater. Res.* (2002) **32**:163.

[4] V. Vaithyanathan, C. Wolverton, and L. Q. Chen, Multiscale modeling of precipitate microstructure evolution. *Phys. Rev. Lett.* (2002) **88**:125503-1.

[5] D. Danilov, B. Nestler, M. Guerdane, and H. Teichler, Bridging the gap between molecular dynamics simulations and phase-field modelling: dynamics of a $[Ni_xZr_{1-x}]_{liquid}$-$Zr_{crystal}$ solidification front. *J. Phys. D: Appl. Phys.* (2009) **42**:015310.

[6] M. Guerdane, F. Wendler, D. Danilov, H. Teichler, and B. Nestler, Crystal growth and melting in NiZr alloy: linking phase-field modeling to molecular dynamics simulations. *Phys. Rev. B* (2010) **81**:224108.

[7] Ch. Hausleitner and J. Hafner, *Phys. Rev. B* (1992) **45**:115.

[8] H. Teichler and M. Guerdane, in *Phase Transformations in multicomponent Melts.* Edited by D. M. Herlach and R. Kirchheim (WILEY-VCH, Weinheim, 2008).

[9] B. Nestler, H. Garcke, B. Stinner, Multicomponent alloy solidification: Phase-field modeling and simulations, *Phys. Rev. E* (2005) **71**:0416091.

[10] M. Guerdane, H. Teichler, and B. Nestler, Local Atomic Order in the Melt and Solid-Liquid Interface Effect on the Growth Kinetics in a Metallic Alloy Model. *Phys. Rev. Lett.* (2013) **110**:086105.